

Effect of temperature and spring-mass systems on modal properties of Timoshenko concrete beam

Hanbing Liu^a, Hua Wang^b, Guojin Tan^{*}, Wensheng Wang^c and Ziyu Liu^d

College of Transportation, Jilin University, Renmin Street No.5988, Changchun 130022, China

(Received July 19, 2017, Revised January 19, 2018, Accepted January 23, 2018)

Abstract. An exact solution for the title problem was obtained in closed-form fashion considering general boundary conditions. The expressions of moment, shear and shear coefficient (or shear factor) of cross section under the effect of arbitrary temperature distribution were first derived. In view of these relationships, the differential equations of Timoshenko beam under the effect of temperature were obtained and solved. Second, the characteristic equations of Timoshenko beam carrying several spring-mass systems under the effect of temperature were derived based on the continuity and force equilibrium conditions at attaching points. Then, the correctness of proposed method was demonstrated by a Timoshenko laboratory beam and several finite element models. Finally, the influence law of different temperature distribution modes and parameters of spring-mass system on the modal characteristics of Timoshenko beam had been studied, respectively.

Keywords: temperature; spring-mass system; mode shape; frequency; Timoshenko beam

1. Introduction

After the structural modal characteristics were found to be sensitive to damage, a significant amount of work has been reported in technical literature regarding the use of changes in modal parameters to identify the location and extent of damage in civil structures. Nowadays, a variety of structural health monitoring methods based on measurement data have been developed for damage detection, among them vibration-based damage identification and condition assessment methods have been mostly widely studies (Cruz and Salgado 2009, Alvandi and Cremona 2006, Talebinejad *et al.* 2011). However, structures are usually subjected to complex environmental conditions which may lead to the variation of modal characteristics (Li *et al.* 2010). A great deal of practical engineering test results has shown that the modal characteristics especially frequencies are susceptible to temperature for concrete structures (Zhou and Yi 2014, Xia *et al.* 2012). Some studies have found that the changes in structural responses due to varying environmental factors could be more significant than those induced by normal structural damage (Salawu 1997). If the effects of temperature are not fully understood, the state of the structure cannot be evaluated reliably (Kim *et al.* 2007). Timoshenko RC beams carrying various concentrated elements (such as linear springs, point masses and spring-mass systems, etc.) are widely used in the civil engineering

structures, such as buildings, bridges, etc. Thus, it is meaningful to study the free vibration analysis of a Timoshenko RC beam carrying multiple spring-mass systems under the effect of temperature.

Extensive research has been carried out with regard to the vibration analysis of Bernoulli-Euler beams carrying concentrated masses as well as spring-mass systems (Rgöze 1985, Liu *et al.* 1988, Register 1994, Kukla and Posiadala 1994, Rosa *et al.* 1995, Gürgöze 1996, Rossit and Laura 2001a, b, Rosa *et al.* 2003, Su and Banerjee 2005). However, the classical one-dimensional Bernoulli-Euler theory of flexural motions of elastic beams has been known to be inadequate for the vibration of higher modes and those beams when the effect of the cross-sectional dimensions on frequencies cannot be neglected (Huang 1961). Therefore, Rayleigh (1945) introduced the effect of rotator inertia and Timoshenko (Timoshenko 1921, 1922) extended it to include the effect of transverse-shear deformation. Since then, a large number of studies on account of Timoshenko theory have been carried out to study free vibration of beams especially with spring-mass system. Bruch and Mitchell (1987) are the ones who presented a uniform cantilever Timoshenko beam carrying a tip mass with lumped mass moment of inertia earlier. Similar works were done by Abramovich and Hamburger (1991, 1992) and Rossi *et al.* (1993). Recently, Farghaly and El-Sayed (2016) dealt with the analysis of the natural frequencies, mode shapes of an axially loaded multi-step Timoshenko beam combined system carrying several attachments. El-Sayed and Farghaly (2016) dealt with the analysis of the vibration of an axially loaded beam system carrying ends consisting of non-concentrated tip masses and three spring-two mass sub-systems.

Over the last several decades, the results of experimental studies (Roberts *et al.* 1996, Wahab and Roeck 1997, He *et*

*Corresponding author, Professor

E-mail: tgj@jlu.edu.cn

^aProfessor

^bPh.D. Student

^cM.Sc.

^dM.Sc.

al. 2009), the primary means ever used, have indicated that temperature is the most significant environmental factor affecting structural modal characteristics. Askegaard and Mossing (1988) studied a three-span RC footbridge and observed a seasonal change of 10% in frequency over a three-year period. Researchers from Los Alamos National Laboratory (Farrar *et al.* 1997, Doebling and Farrar 1997, Cornwell *et al.* 1999) performed several tests on the Alamosa Canyon Bridge and found that the first three natural frequencies varied about 4.7%, 6.6% and 5.0% during a 24h period as the temperature of the bridge deck changed by approximately 22 °C. The Z24 bridge in Switzerland was monitored over almost one year by Peeters *et al.* (2000, 2001). The first four natural frequencies varied by 14%-18% as the changing environmental conditions while decreased by less than 10% till the final damage scenario (Maeck *et al.* 2000). Li *et al.* (2010) found that the first six frequencies varied by about 1.5-3.2% as ambient temperature changing from -11.5 to 3.7°C. Faravelli *et al.* (2011) observed variations in frequencies of the 600 m Guangzhou New TV Tower during a 24 h period. As variations in ambient temperature were about only 3 °C, variations in frequencies were as small as 0.5%. Kim *et al.* (2007) carried out laboratory tests on a steel plate-girder bridge model. The first four frequencies decreased by about 0.64, 0.33, 0.44, and 0.22%, respectively, when temperature increased per unit degree.

Since the discovery of temperature has obviously influence on structural modal characteristics, some methods have proposed for analyzing the relationship between them. Statistical techniques are widely applied to describe the relation between temperature and modal properties, which hoped to eliminate the temperature-induced variation of modal characteristics from the measured ones. Sohn *et al.* (1999) proposed a linear adaptive model (multiple linear regression model) to discriminate the changes of modal frequencies due to temperature from those caused by structural damage or other environmental effects. Peeters and De Roeck (2000) subsequently trained an autoregressive model with an exogeneous input (ARX) using the one-year monitoring data of Z24 bridge to distinguish normal modal frequency changes due to environmental effects from abnormal changes caused by damage. The support vector machine (SVM) technique (Ni *et al.* 2005) and principal component analysis (PCA) (Yan 2005a, b) were also adopted to quantify the effect of temperature on modal frequencies. Xia *et al.* (2006, 2011) conducted a series of experiments to find the relationship of temperature and structural modal characteristics. In Reference (Xia *et al.* 2006), they constructed a two-span RC slab and built a linear regression model between modal properties and air temperature. It was found that frequency does not vary with temperature simultaneously for the variation of internal temperature of a structure lags behind the variation of the surface or air temperature. Later, an improved numerical method considering non-uniform temperature distribution was represented in Reference (Xia *et al.* 2011). A good linear correlation between the measured natural frequencies and the structural temperatures other than the air temperature or surface temperatures was observed. Liu *et al.* (2016) also proposed multiple linear regression models considering non-uniform

temperature distribution and suggested that the variation of concrete Young's modulus with temperature was the main reason resulting in the changes of modal frequencies.

In summary, it has been widely observed that temperature variation has an enormous effect on structural modal characteristics through situ-test and laboratory. In addition, most of the researches focus on the statistical techniques (i.e., regression models, autoregressive models, principal component analysis, etc.), numerical models and experimental methods to establish the correlation between temperature and modal characteristics. However, these models and methods apply only to specific objects and are relatively narrow. It needs to investigate the internal mechanism of modal characteristics change induced by temperature and form a calculated method of modal characteristics based on the basic theory of kinetics equations for structures under the effect of temperature.

For most of the construction materials, it is generally accepted that an increase in temperature will cause a decrease in Young's modulus and the shear modulus of the materials (Xia *et al.* 2011), which was considered to be the main reason for the change of structural modal characteristics (Liu *et al.* 2016). Moreover, the temperature distribution in a structure is generally non-uniform and time dependent. Therefore, Young's modulus throughout a structure with existence of temperature gradient is not identical. Under this concept, a new method was proposed for Timoshenko beam carrying several spring-mass systems under the effect of arbitrary temperature distribution of cross section. This method was featured by the following points: first, the expressions of moment, shear and shear coefficient of cross section under the effect of arbitrary temperature distribution were derived; second, in view of these relationships the differential equations of Timoshenko beam under the effect of temperature were obtained and solved; then, the characteristic equations of Timoshenko beam carrying several spring-mass systems under the effect of temperature were formed based on the continuity and force equilibrium conditions at attaching points; the correctness of proposed method was next verified by a Timoshenko laboratory beam and finite element models; finally, the influence law of different temperature distribution modes and parameters of spring-mass system on the modal characteristics of Timoshenko beam were discussed.

2. Derivations of moment, shear and shear coefficient of cross section under the effect of temperature

Young's modulus E is related to the temperature according to reference (Xia *et al.* 2011) by

$$E = E_0(1 - \theta_E T_p) \quad (1)$$

where E_0 is Young's modulus of concrete at 0°C, T_p is Celsius temperature, θ_E is temperature coefficient (or thermal coefficient) of Young's modulus, which is suggested as 0.0045 by Baldwin and North's report (Baldwin and North 1973).

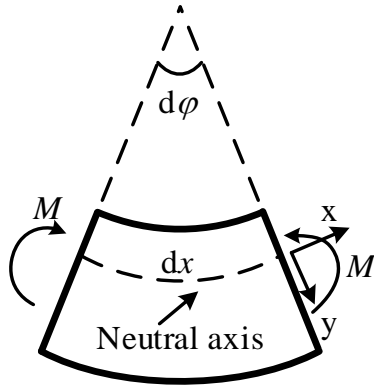


Fig. 1 Deformation of micro segment subjected to bending moment M

According to Eq. (1), Young's modulus decreases with increasing temperature, which agrees with macroscopic observations of the variations of eigenfrequencies of test concrete beams and slabs (e.g., Xia *et al.* 2011, Liu *et al.* 2016) subjected to changes in temperature.

It is assumed that temperature distributions along the length and width of the Timoshenko RC beam are identical. Then Eq. (1) after substituting the distribution function $T(y)$ of the temperature along the cross-sectional height becomes

$$E(y) = E_0[1 - \theta_E T(y)] = E_0 f(y) \quad (2)$$

where $f(y) = 1 - \theta_E T(y)$.

Fig. 1 shows the deformation of micro segment dx subjected to bending moment M along the z -axis.

Strain $\varepsilon(y)$ and M could be expressed as follows

$$\varepsilon(y) = -\frac{d\phi}{dx} y \quad (3)$$

$$M = \int_A \sigma(y) y dA \quad (4)$$

Substituting Eqs. (2)-(3) into Eq. (4) gives

$$M = -\int_A \frac{d\phi}{dx} E(y) y^2 dA = -\frac{d\phi}{dx} E_0 I_T \quad (5)$$

where $I_T = \int_A f(y) y^2 dA$.

According to the combination of Eqs. (2) (3) and (5), one obtains

$$\sigma(y) = \frac{M f(y) y}{I_T} \quad (6)$$

A micro segment, the part in Fig. 1 below the plane at y which was parallel to the neutral plane, was shown in Fig. 2, where b is the cross-sectional width, F_{N1} and F_{N2} are axial force, τ is shearing stress along the y -axis while τ' is shearing stress along the x -axis. Then the equilibrium equation of force along x -axis is

$$F_{N1} + \tau' b dx = F_{N2} \quad (7)$$

where F_{N1} is

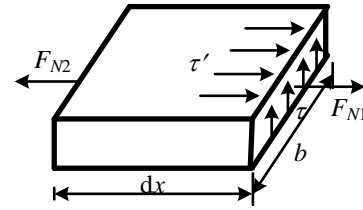


Fig. 2 Force analysis of the micro segment

$$F_{N1} = \int_{A^*} \sigma dA \quad (8)$$

Substituting Eq. (6) into Eq. (8) yields

$$F_{N1} = \int_{A^*} \frac{M f(y) y}{I_T} dA \quad (9)$$

Similarly,

$$F_{N2} = \int_{A^*} \frac{(M + dM) f(y) y}{I_T} dA \quad (10)$$

Let

$$S^*(y) = \int_{A^*} f(y) y dA \quad (11)$$

According to the equivalent law of shearing stress (i.e., $\tau' = \tau$) and substituting Eqs. (9)-(10) into Eq. (7) results in

$$\tau(y) = \frac{dM}{dx} \frac{S^*(y)}{b I_T} \quad (12)$$

which after substituting $dM/dx = Q$ becomes

$$\tau(y) = \frac{Q S^*(y)}{b I_T} \quad (13)$$

Concrete assumed as isotropic material, with the following relationship holds

$$G = \frac{E}{2(1+\nu)} \quad (14)$$

The effect of temperature on Poisson's ratio of concrete seems negligible when the temperature ranges from -20°C to $+50^\circ\text{C}$ (Shoukry *et al.* 2011). Therefore substituting Eq. (2) into Eq. (14) gives

$$G(y) = G_0(1 - \theta_E T) = G_0 f(y) \quad (15)$$

Average shear modulus G_T , average shear stress τ_T and average shear strain γ_T are defined as follows

$$G_T = \frac{\int G(y) dA}{A}, \quad \tau_T = \frac{Q(x)}{A}, \quad \gamma_T = \frac{\tau_T}{k_T G_T} \quad (16)$$

where k_T is the shear coefficient (or shape factor) for the cross section.

Strain energy U_1 of cross section is related to G_T and γ_T by

$$U_1 = \frac{k_T}{2} G_T A \gamma_T^2 \tag{17}$$

While the strain energy of the cross section can also be expressed as

$$U_2 = \int_A \frac{\tau^2(y)}{2G(y)} dA \tag{18}$$

Inserting Eqs. (13) and (16) into Eqs. (18) and let $U_1=U_2$ yields

$$k_T = \frac{b^2 I_T^2}{\int_A \frac{S^{*2}(y)}{f(y)} dA \int_A f(y) dA} \tag{19}$$

Then Q can be written as

$$Q = k_T G_0 A_T \gamma_T \tag{20}$$

where $A_T = \int_A f(y) dA$.

3. Free vibration analysis of Timoshenko beam under the effect of varied temperature

As it is well-known, when temperature variation $T(y)$ is non-linear along the thickness of the cross-section, it caused a stress state with zero resultants even though the structure is statically determined. The statically undetermined structures especially beams with axial constraints were not considered in this paper.

When the Timoshenko beam vibrates in one of its normal modes one can assume free vibration of the beam takes the following form

$$y(x, t) = Y(\xi) e^{i\omega t} \tag{21}$$

$$\phi(x, t) = \psi(\xi) e^{i\omega t} \tag{22}$$

where ω is angular frequency, $i = \sqrt{-1}$, $\xi = x/L$ is the non-dimensional coordinate normalized with respect to the beam length L , then $Y(\xi)$ and $\psi(\xi)$ denote the amplitudes of total deflection $y(x, t)$ and rotation $\phi(x, t)$ of the cross-section, respectively.

Taking into account bending moment and shear force of Eqs. (5) and (20), the problem under consideration, similarly to reference (Abramovich and Elishako 1990), is governed by the following differential equations

$$Y^{(4)} + p^2(r^2 + b^2)Y'' - p^2Y = 0 \tag{23}$$

$$\psi^{(4)} + p^2(r^2 + b^2)\psi'' - p^2\psi = 0 \tag{24}$$

where

$$p^2 = \frac{\rho A \omega^2 L^4}{E_0 I_T} \tag{25}$$

$$r^2 = I / (A L^2) \tag{26}$$

$$b^2 = E_0 I_T / (k_T A_T G_0 L^2) \tag{27}$$

ρ is the beam material density, I is the cross-sectional moment of inertia and the prime denotes differentiation with respect to ξ .

The general solutions of Eqs. (23)-(24) are

$$Y(\xi) = C_1 \cosh p\alpha\xi + C_2 \sinh p\alpha\xi + C_3 \cos p\beta\xi + C_4 \sin p\beta\xi \tag{28}$$

$$\psi(\xi) = C'_1 \cosh p\alpha\xi + C'_2 \sinh p\alpha\xi + C'_3 \cos p\beta\xi + C'_4 \sin p\beta\xi \tag{29}$$

where $\alpha = \frac{1}{\sqrt{2}} \left\{ -(r^2 + b^2) + [(r^2 + b^2)^2 + 4/p^2]^{1/2} \right\}^{1/2}$,

$\beta = \frac{1}{\sqrt{2}} \left\{ (r^2 + b^2) + [(r^2 + b^2)^2 + 4/p^2]^{1/2} \right\}^{1/2}$.

One just needs to know half of the constants in Eqs. (28)-(29) for they are related as

$$C'_1 = \delta_1 C_2, \quad C'_2 = \delta_1 C_1, \quad C'_3 = \delta_2 C_4, \quad C'_4 = -\delta_2 C_3.$$

where $\delta_1 = \frac{p}{L} \frac{\alpha^2 + b^2}{\alpha}$, $\delta_2 = \frac{p}{L} \frac{\beta^2 - b^2}{\beta}$.

4. Vibration analysis of Timoshenko beam carrying several spring-mass systems under the effect of temperature

Fig. 3 shows a uniform Timoshenko beam elastically supported carrying N spring-mass systems. The i th spring-mass system was located at x_i , where x_i is the spatial coordinate along the length of beam L . Then the whole beam is divided into $N+1$ segments by N spring-mass systems. z_i , m_i , and k_i are displacement, mass and spring stiffness of the i th spring-mass system, respectively; k_{z1} and k_{z2} are the translational stiffness while k_{z3} and k_{z4} are rotational stiffness.

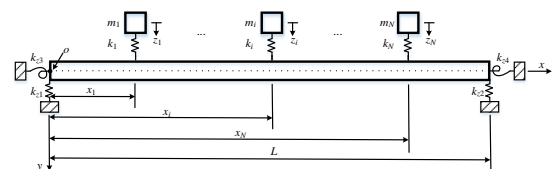


Fig. 3 A uniform Timoshenko beam elastically supported carrying N spring-mass systems

For the i th segment which was divided by the i th spring-mass system, let $\xi = x/L$ according to Eqs. (28)-(29), one has

$$Y_i(\xi) = A_i \cosh p\alpha\xi + B_i \sinh p\alpha\xi + C_i \cos p\beta\xi + D_i \sin p\beta\xi \tag{30}$$

$$\psi_i(\xi) = A_i \delta_1 \sinh p\alpha\xi + B_i \delta_1 \cosh p\alpha\xi - C_i \delta_2 \sin p\beta\xi + D_i \delta_2 \cos p\beta\xi \quad (31)$$

where $\xi_{i-1} \leq \xi \leq \xi_i$ ($i=1, 2, \dots, N+1$, and $\xi_0=0, \dots, \xi_i = x_i/L, \dots, \xi_{N+1}=1$), i denotes the i th “attaching point” and A_i, B_i, C_i and D_i are the integration constants.

4.1 Equations at the i th attaching point

The continuity equations of the beam at the position $\xi = \xi_i$ are

$$Y_i(\xi_i) = Y_{i+1}(\xi_i) \quad (32a)$$

$$\psi_i(\xi_i) = \psi_{i+1}(\xi_i) \quad (32b)$$

$$\psi'_i(\xi_i) = \psi'_{i+1}(\xi_i) \quad (32c)$$

The equation of motion for the i th spring-mass system is

$$k_i [(y_i(\xi_i, t) - z_i(t))] - m_i \ddot{z}_i = 0 \quad (33)$$

Similar to Eq. (21), free vibration of the i th spring-mass system is assumed as

$$z_i(t) = Z_i e^{i\omega t} \quad (34)$$

where Z_i is the amplitude of the i th spring-mass system.

Substituting Eqs. (21) and (34) into Eq. (33) gives

$$Y_i(\xi_i) + (\gamma_v^2 - 1)Z_i = 0 \quad (35)$$

where

$$\gamma_v^2 = \frac{\omega^2}{\omega_v^2} \quad (36)$$

$$\omega_v = \sqrt{k_i / m_i} \quad (37)$$

From the force equilibrium at $\xi = \xi_i$, one has

$$kG_0 A_T (\psi_i(\xi_i) - Y'_i(\xi_i)/L - \psi_{i+1}(\xi_i) + Y_{i+1}(\xi_i)/L) + F_m = 0 \quad (38)$$

where F_m is the interactive force between the beam and the i th spring-mass system, it can be given by

$$F_m = k_i \frac{\gamma_v^2}{1 - \gamma_v^2} Y_i(\xi_i) \quad (39)$$

The substitution of Eqs. (30)-(31) into Eqs. (32), (35), and (38) leads to

$$[T_i] \{I_i\} = 0 \quad (40)$$

where

$$I_i = \{A_i \ B_i \ C_i \ D_i \ Z_i \ A_{i+1} \ B_{i+1} \ C_{i+1} \ D_{i+1}\}^T \quad (41a)$$

$$T_i = \begin{bmatrix} S_{i-4} & S_{i-3} & S_{i-2} & S_{i-1} & S_i & S_{i+1} & S_{i+2} & S_{i+3} & S_{i+4} \\ \eta_1 & \eta_2 & \eta_3 & \eta_4 & 0 & -\eta_1 & -\eta_2 & -\eta_3 & -\eta_4 \\ \delta_1 \eta_2 & \delta_1 \eta_1 & -\delta_2 \eta_4 & \delta_2 \eta_3 & 0 & -\delta_1 \eta_2 & -\delta_1 \eta_1 & \delta_2 \eta_4 & -\delta_2 \eta_3 \\ \delta_1 p \alpha \eta_1 & \delta_1 p \alpha \eta_2 & -\delta_2 p \beta \eta_3 & -\delta_2 p \beta \eta_4 & 0 & -\delta_1 p \alpha \eta_1 & -\delta_1 p \alpha \eta_2 & \delta_2 p \beta \eta_3 & \delta_2 p \beta \eta_4 \\ \epsilon_1 \eta_2 + \lambda \eta_1 & \epsilon_1 \eta_1 + \lambda \eta_2 & -\epsilon_2 \eta_4 + \eta_3 & \epsilon_2 \eta_3 + \eta_4 & \gamma_v^2 - 1 & 0 & 0 & 0 & 0 \end{bmatrix} \quad (41b)$$

where $\eta_1 = \cosh(p\alpha\xi_i)$, $\eta_2 = \sinh(p\alpha\xi_i)$, $\eta_3 = \cos(p\beta\xi_i)$, $\eta_4 = \sin(p\beta\xi_i)$, $\epsilon_1 = \delta_1 L - p\alpha$, $\epsilon_2 = \delta_2 L - p\beta$, $\lambda = \frac{k_i L \gamma_v^2}{k_T G_0 A_T (1 - \gamma_v^2)}$.

4.2 Equations at the ends of the beam

At the condition of $\xi = 0$, the left boundary conditions are

$$kG_0 A_T (\psi(0) - Y'(0)/L) + k_{z1} Y(0) = 0 \quad (42a)$$

$$-E_0 I_T \psi'(0) + k_{z3} Y'(0) = 0 \quad (42b)$$

At the condition of $\xi = 1$, the right boundary conditions are

$$-kG_0 A_T (\psi(1) - Y'(1)/L) + k_{z2} Y(1) = 0 \quad (43a)$$

$$E_0 I_T \psi'(1) + k_{z4} Y'(1) = 0 \quad (43b)$$

Hence from Eqs. (30), (31) (42) and (43) one can obtain

$$[T_L] \{I_L\} = 0 \quad (44a)$$

$$[T_R] \{I_R\} = 0 \quad (44b)$$

where

$$T_L = \begin{bmatrix} 1 & 2 & 3 & 4 \\ k_{z1} L & kG_0 A_T \epsilon_1 & k_{z1} L & kG_0 A_T \epsilon_2 \\ -E_0 I_T \delta_1 \alpha_1 & k_{z3} \alpha_1 & E_0 I_T \delta_2 \beta & k_{z3} \beta_1 \end{bmatrix} \quad (45a)$$

$$T_R = \begin{bmatrix} 5N+1 & 5N+2 & 5N+3 & 5N+4 \\ k_{z2} L \eta_5 - \epsilon_1 \eta_6 & k_{z2} L \eta_6 - \epsilon_1 \eta_5 & k_{z2} L \eta_7 - \epsilon_2 \eta_8 & k_{z2} L \eta_8 - \epsilon_2 \eta_7 \\ kG_0 A_T & kG_0 A_T & kG_0 A_T & kG_0 A_T \\ k_{z4} \omega \eta_6 + E_0 I_T \alpha \delta_1 \eta_5 & k_{z4} \omega \eta_5 + E_0 I_T \alpha \delta_1 \eta_6 & -k_{z4} \beta \eta_8 - E_0 I_T \beta \delta_2 \eta_7 & k_{z4} \beta \eta_7 + E_0 I_T \beta \delta_2 \eta_8 \end{bmatrix} \quad (45b)$$

$$\{I_L\} = \{A_1 \ B_1 \ C_1 \ D_1\} \quad (45c)$$

and

$$\{I_R\} = \{A_{N+1} \ B_{N+1} \ C_{N+1} \ D_{N+1}\} \quad (45d)$$

where $\eta_5 = \cosh(p\alpha)$, $\eta_6 = \sinh(p\alpha)$, $\eta_7 = \cos(p\beta)$, $\eta_8 = \sin(p\beta)$.

For three general boundary conditions, one only needs to change the values of $k_{z1}-k_{z4}$ in Eq. (44), i.e.,

(1) Simply supported beam

$$k_{z1} \rightarrow \infty, \ k_{z2} \rightarrow \infty, \ k_{z3} = 0, \ k_{z4} = 0 \quad (46)$$

(2) Clamped-clamped beam

$$k_{z1} \rightarrow \infty, \ k_{z2} \rightarrow \infty, \ k_{z3} \rightarrow \infty, \ k_{z4} \rightarrow \infty \quad (47)$$

(3) Cantilever beam

$$k_{z1} \rightarrow \infty, k_{z2} = 0, k_{z3} \rightarrow \infty, k_{z4} = 0 \quad (48)$$

4.3 Solutions of eigenvalues and mode shapes

Note that the total number of equations are $5N+4$ (including $5N$ equations at N attaching points and 2 equations at each boundary) in the case of a Timoshenko beam carrying N spring-mass systems. The right numbers and top numbers, as shown on the right side and top side of the matrix defined by Eqs. (41b), (45a) and (45b), represent the line numbers and column numbers of corresponding elements in an overall matrix $[\bar{T}]$. Accordingly, one can take $[T_i]$, $[T_L]$ and $[T_R]$ in an overall matrix $[\bar{T}]$ and replace the $5N+4$ equations as

$$[\bar{T}]\{\bar{T}\} = 0 \quad (49)$$

where

$$\{\bar{T}\} = \{A_1, B_1, C_1, D_1, Z_1, \dots, A_i, B_i, C_i, D_i, Z_i, \dots, A_{N+1}, B_{N+1}, C_{N+1}, D_{N+1}\} \quad (50)$$

Non-triviality condition of the problem requires that

$$\det(\bar{T}) = 0 \quad (51)$$

As Eq. (51) is a complicated function of ω . The half-interval technique (Faires and Burden 2002) may be used to obtain the eigen-values ω_i ($i=1, 2, \dots$). Then one can take each ω_i in Eq. (49) and derive the values of $\{\bar{T}\}$. Among the Eqs. (30)-(31), the corresponding mode shapes $Y_i(\xi)$ and $\psi_i(\xi)$ could be obtained. Eq. (49) also applies to the Timoshenko beam without any spring-mass systems, only when the mass of the spring-mass systems are zero.

5. Experiment results and parameter discussions

5.1 Comparison with the experiment

A simply supported RC beam, as an illustrated model shown in Fig. 4, was constructed on 25th June, 2015 which measures 400 cm long, 30 cm wide and 40 cm high with 15 cm overhang at each end. Two laminated rubber bearings were chosen as supports. Grade C40 concrete was selected in accordance with the GB 50010-2010 (2010). The length of beam is much larger than its height and width and solar intensity along the length direction of beam is uniform, so temperature along the length direction could be assumed to be uniformly distributed. Seven thermocouples embedded in the cross section of mid-span were uniformly-spaced along the width as well as height before pouring concrete, as shown in Fig. 5.

After the beam curing 28 days, modal tests were carried out. The beam was excited by an impact hammer and the vibration responses were collected by 2 accelerometers in the positions shown in Fig. 6. Then DH5922 system produced by DongHua Testing Technology Company Limited sampled about 24-second data at a sampling rate of

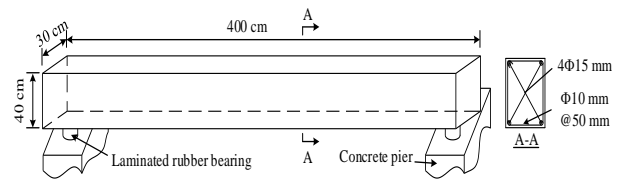


Fig. 4 The simply supported RC Timoshenko beam

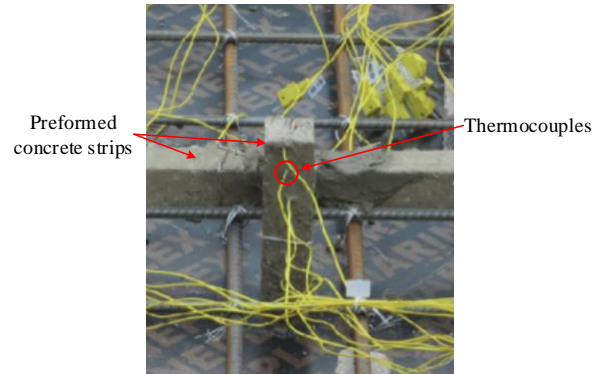


Fig. 5 Positioning thermocouples inside the beam

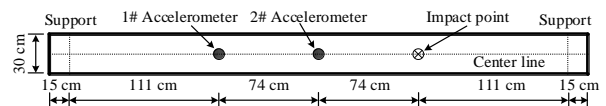


Fig. 6 Accelerometers layout on the RC Timoshenko beam

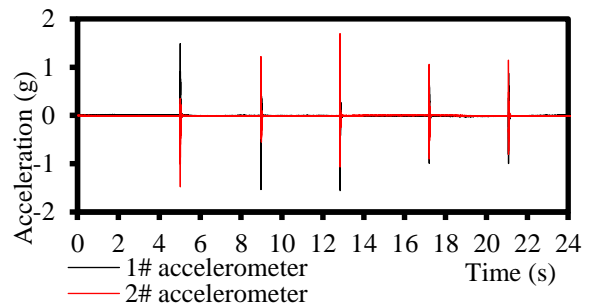


Fig. 7 Acceleration time-history curves on 18th September 2016 at 8:00 am

5120 Hz. The first three modal frequencies were extracted by the Hilbert-Huang Transform (HHT) which is a popular time-frequency method.

The test aims to investigate the variation of the structural modal characteristics with respect to different temperatures. Accordingly, a 24-hour modal testing was carried out hourly from 8:00 am on 18th September, 2016 (Fig. 7 shows acceleration time-history curves on 18th September 2016 at 8:00 am and the corresponding lowest three modal frequencies extracted by HHT are shown in Fig. 8). Meanwhile, the temperatures were automatically recorded by TP700 data recorder at a rate of one sample per minute (Fig. 9 shows variation of test temperature at cross-sectional centre point in a 24-hour period). According to the measured temperature and the relationship between the Young's modulus and temperature in Eq. (2), the modal frequencies of beam could be calculated by solving the dynamic Eq. (49).

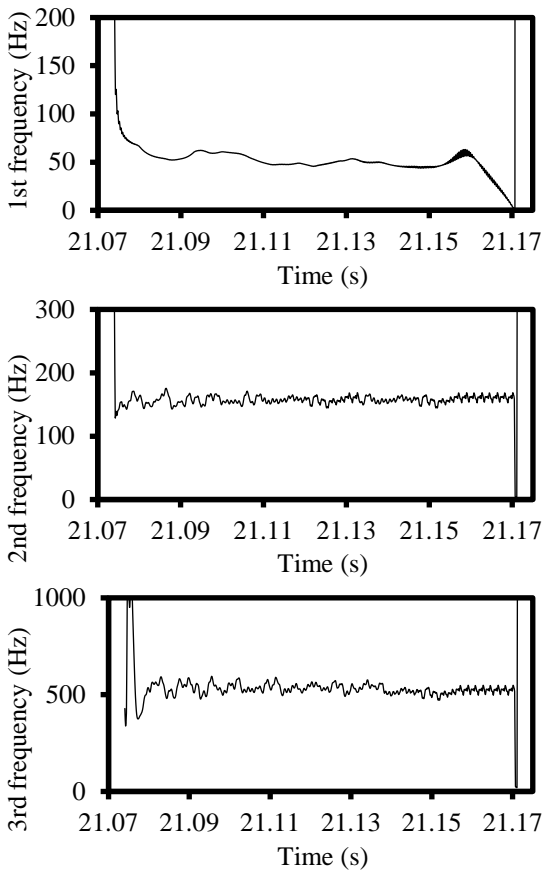


Fig. 8 The lowest three frequencies on 18th September 2016 at 8:00 am

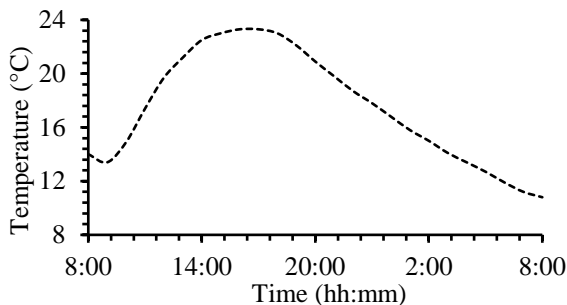


Fig. 9 Variation of test temperature at cross-sectional centre point in a 24-hour period

As the Young's modulus used in the proposed method are not exactly the same as the real ones, the calculated frequencies differ from the measurements. To validate the proposed method the variation ratios of frequency (*FVR*) between test and calculation results are compared and plotted in Fig. 10. *FVR* is defined as

$$FVR = \frac{\omega_i}{\omega_0} \times 100\% \quad (52)$$

where ω_i is the frequency at time i , ω_0 is the frequency at initial time, i.e., 8:00 am on 18th September.

The results referring to Euler model could be easily obtained when the moment of inertia and shear deformation of the cross section are ignored. And the results are also

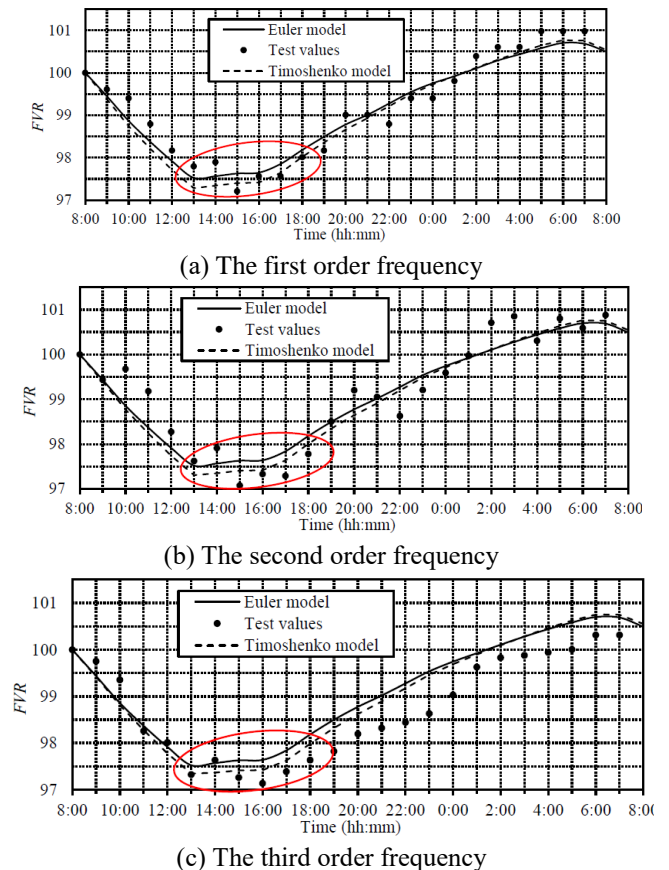


Fig. 10 Comparison of the frequency variations between the test values, Euler and Timoshenko model at different times

plotted in Fig. 10 for comparative purposes.

The *FVR* based on Timoshenko model showed good agreement with test values as well as Euler model, which verifies correctness of the proposed method with respect to variation of temperature.

It should be noted that *FVR* obtained by Timoshenko model are very close to those of Euler model when temperature changed little. However, there are some differences at a time (e.g., the areas in the red circle in Fig. 10) when temperature changed more obviously (see Fig. 9). And the results of Timoshenko model maybe closer than those of Euler model (e.g. from 15:00 to 19:00 in Fig. 10(a), from 15:00 to 18:00 in Fig. 10(b) and from 15:00 to 22:00 in Fig. 10(c)).

5.2 Comparison with FEM results

In order to check the reliability of the theory presented, the lowest three frequencies and modal shapes of Timoshenko beam carrying one, two and three spring-mass systems are compared with FEM, respectively. The dimensions and physical properties of the Timoshenko beam are given as: length of beam is 5 m, cross-sectional width is 0.2 m, cross-sectional height is 0.5 m, Young's modulus $E_0=3.25 \times 10^{10}$ MPa at 0 °C, Poisson ratio $\nu=0.3$, mass density of beam material is 2500 kg/m³.

2D finite element models in ANSYS shown in Fig. 11 are constructed by axial symmetry element PLANE 183.

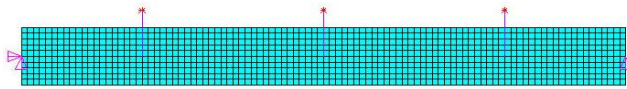


Fig. 11 Finite element model of a simply supported Timoshenko beam carrying three spring-mass systems

Table 1 Lowest three frequencies of bare beam carrying zero, one, two and three spring-mass systems compared with FEM

Locations of spring-mass systems	Magnitudes of masses (kg)	Magnitudes of springs' stiffness (N/m)	Method	Natural frequencies(Hz)			
				f_1	f_2	f_3	
Case 1	Bare beam		Present	32.13	122.74	257.21	
			FEM	32.09	121.97	255.04	
				(0.0012)	(0.0063)	(0.0085)	
Case 2	$\zeta_1=0.5$	$m_1=100$	$k_1=3.24 \times 10^6$	Present	36.88	122.74	257.86
				FEM	36.84	121.97	255.28
				(0.0012)	(0.0063)	(0.0101)	
Case 3	$\zeta_1=0.2$ $\zeta_2=0.6$	$m_1=100$ $m_2=100$	$k_1=3.24 \times 10^6$ $k_2=3.24 \times 10^6$	Present	37.67	123.42	257.92
				FEM	37.64	122.66	255.35
				(0.0009)	(0.0062)	(0.0101)	
Case 4	$\zeta_1=0.2$ $\zeta_2=0.5$ $\zeta_3=0.8$	$m_1=100$ $m_2=100$ $m_3=100$	$k_1=3.24 \times 10^6$ $k_2=3.24 \times 10^6$ $k_3=3.24 \times 10^6$	Present	38.91	123.73	258.30
				FEM	38.88	122.97	255.72
				(0.0008)	(0.0062)	(0.0101)	

Table 2 The first three frequencies of the Timoshenko beams of different models

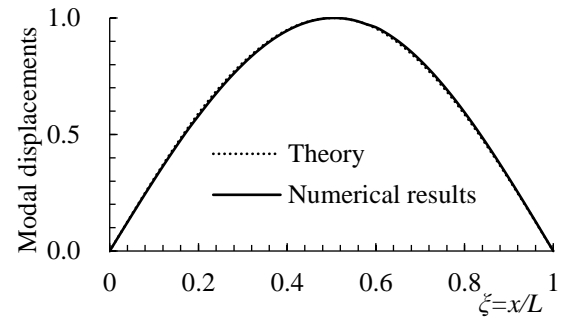
Different model	1 st (Hz)	2 nd (Hz)	3 rd (Hz)
Bare beam	32.13	122.74	257.21
Temperature=20°C	30.67 Relative (-0.045)	117.09 relative (-0.046)	245.73 relative (-0.045)
Single spring-mass system	33.54 Relative (0.044)	122.74 Relative (0.000)	257.73 Relative (0.002)

The temperature distribution in the modal is identical and 0°C was adopted. The parameters of the spring-mass system are shown in Table 1. These are inputted into the ANSYS model to calculate the modal characteristics. For convenience, Timoshenko beam without any spring-mass systems attached and under the effect of a uniform temperature distribution of 0°C was referred to the bare beam.

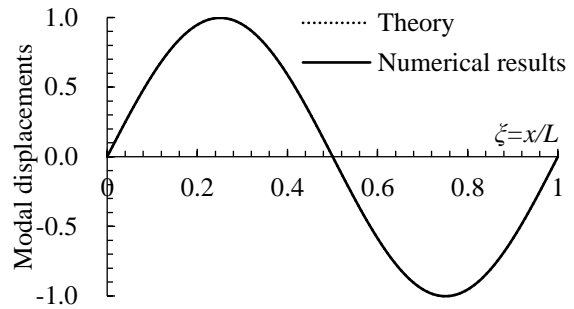
From Table 1 and Fig. 12, one can see that the lowest three frequencies and modal shapes of the Timoshenko beam obtained from the present study are very close to those calculated by FEM, which verifies correctness of the proposed method for Timoshenko beam carrying several spring-mass systems.

5.3 The effect of temperature variation and spring-mass system on modal frequencies of Timoshenko beam

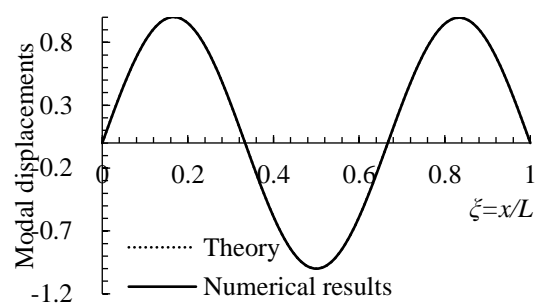
The parameters of the Timoshenko beam adopted in last



(a) The first modal shape



(b) The second modal shape



(c) The third modal shape

Fig. 12 Comparison of the first three modal shapes between theory and numerical results for the Timoshenko beam carrying two spring-mass systems

section were used here as well as following parts. Table 2 shows the first three frequencies of the Timoshenko beams of different models: (a) the bare beam; (b) the temperature changes from 0°C to 20°C; (c) the bare beam carrying single spring-mass system with $\zeta=0.5$, stiffness $k=1.5 \times 10^6$ N/m and mass $m=100$ kg.

As can be seen from Table 2, the first three frequencies of the Timoshenko beam are reduced by about 4.5% when the temperature varies from 0 to 20°C. The first order frequency of the Timoshenko beam increases by 4.4% while the other two do not change substantially when the bare beam carrying one spring-mass system. One can see that the effects of temperature and spring-mass systems on modal frequencies of Timoshenko beam are both of significance and the latter has different effects on different order frequencies.

5.4 The effect of different parameters of single spring-mass system on modal characteristics of Timoshenko beam

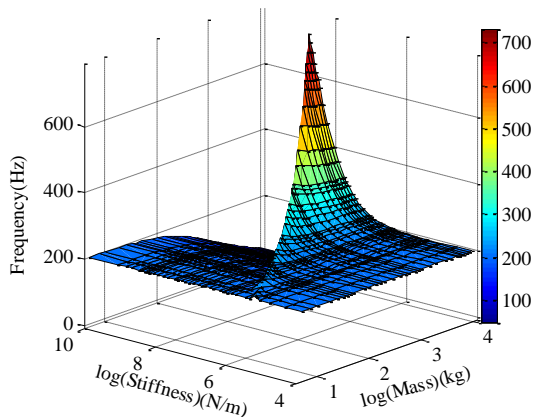
For convenient, the Timoshenko beam which has

uniform material properties carries single spring-mass system located at mid-span was adopted. Then the modal frequencies were calculated by the proposed method with respect to different parameters of spring-mass system. The first-order frequency varies with the stiffness and mass of the spring-mass systems as shown in Fig. 13(a), where the stiffness and mass are logarithmic. The parameters of spring-mass system are divided into two regions A and B, as shown in Fig. 13(b) (the top view of Fig. 13(a)). From Fig. 13 one could see: (a) in region A, the frequencies were less than those of the bare beam while region B were opposite; (b) the frequencies increase with the stiffness while decrease with the mass both in A and B; (c) a change of frequencies appeared suddenly at the line where A and B meet. The fitting formula of the line in Fig. 14 is

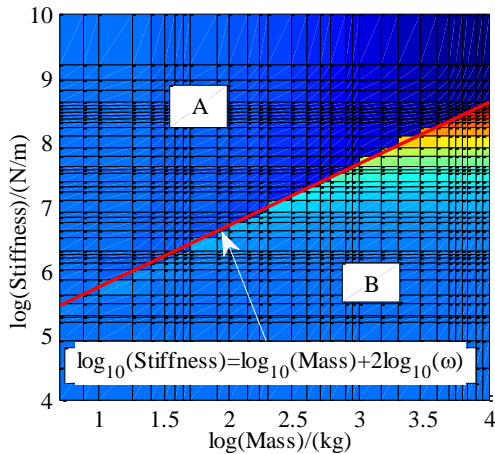
$$\frac{Stiffness}{Mass} = \omega^2 \tag{53}$$

From Eqs. (37) and (53) one has $\omega_v = \omega$, which indicates that when the frequency of the spring-mass system is equal to that of the bare beam, the frequency of the Timoshenko beam carrying one spring-mass system changes abruptly.

In particular, the spring-mass system has no effect on the second order frequency due to it locates at the zero point of the second modal shape for simply supported beam.



(a) Axonometric view



(b) Overhead view

Fig. 13 The first order frequency varies with the stiffness and mass

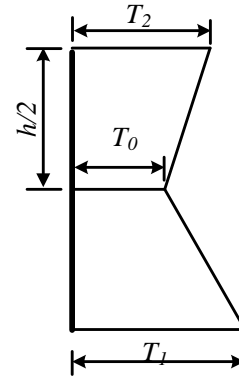


Fig. 14 Temperature distribution along the height of cross section

5.5 The effect of different temperature modes on modal frequencies of Timoshenko beam

In Fig. 14, T_0 , T_1 and T_2 represent the temperature at $h/2$, the lower edge and the upper edge of the cross section, respectively. The intermediate temperature is linearly interpolated and the following three temperature modes are defined as: (1) mode A, $T_1=-20^\circ\text{C}$, T_2 changes from -20°C to 40°C and $T_0=(T_1+T_2)/2$; (2) mode B, $T_0=10^\circ\text{C}$, T_2 changes from -20°C to 40°C and $T_1=2T_0-T_2$; (3) mode C, $T_0=10^\circ\text{C}$, T_2 changes from -20°C to 40°C and $T_1=T_2$.

Characteristics of cross section varying with T_2 under different temperature modes are shown in Fig. 15, where the variance ratio of shearing factor (SVR) is defined as

$$SVR = \frac{SF_T - SF_0}{SF_0} \times 100\% \tag{54}$$

where SF_T and SF_0 are the shear coefficients at temperature T_2 and -20°C , respectively.

The variance ratio of I_T (IVR) is defined as

$$IVR = \frac{I_{TT} - I_{T0}}{I_{T0}} \times 100\% \tag{55}$$

where I_{TT} and I_{T0} are moment of inertia at temperature T_2 and -20°C , respectively.

It can be seen that SVR and IVR change with the temperature distribution. SVR in mode A and B have changed little while that in mode C is up to 5%. IVR in mode A and C changed obviously which are basically linear while that in mode B is small.

Fig. 16 shows a Timoshenko beam carrying two spring-mass systems, where $x_1=1\text{ m}$, $x_2=3\text{ m}$, $k_1=k_2=3.24 \times 10^6\text{ N/m}$ and $m_1=m_2=100\text{ kg}$. FVR under different temperature modes are obtained in Fig. 17.

As can be seen from Fig. 17: (1) FVR changes with temperature, while the second and third FVR changed more obviously than the first one; (2) FVR in mode A and C changed similarly, while that in mode B varied less than that in the other two. Therefore, it could conclude that the influence of different temperature modes on frequency is different. In addition, the temperature has different effect on every frequency in the same temperature mode.

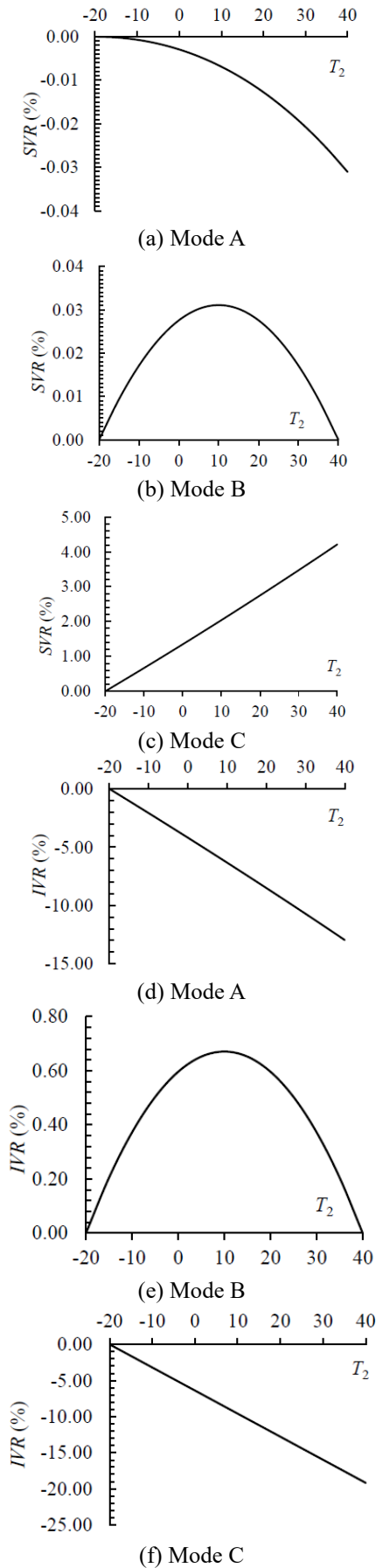


Fig. 15 Characteristics (SVR and IVR) of cross section varying with T_2 under different temperature modes

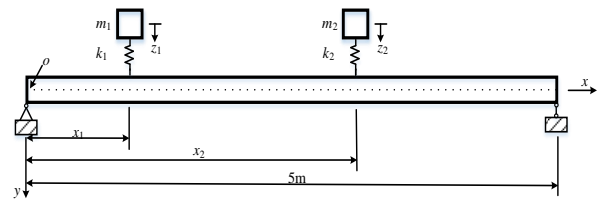


Fig. 16 A simply supported Timoshenko beam carrying two spring-mass systems

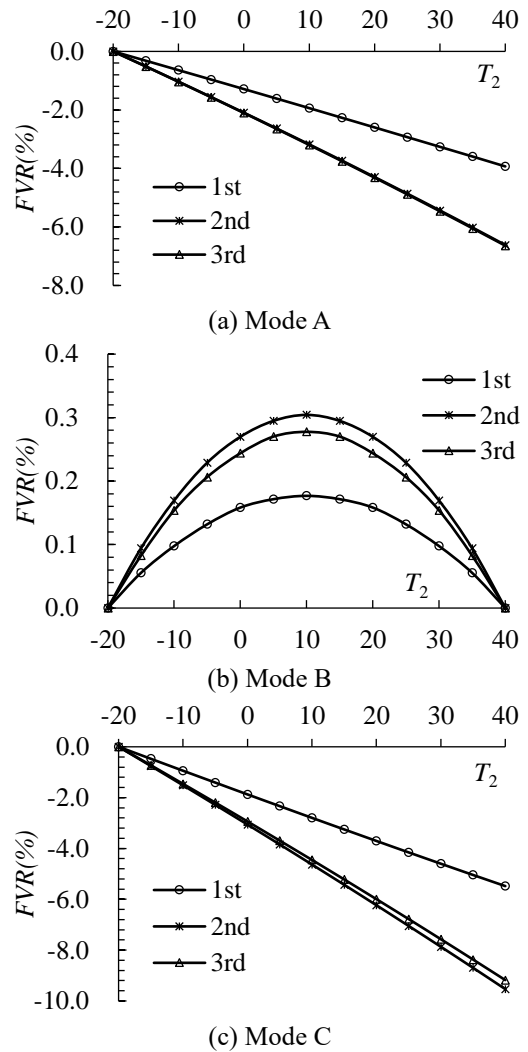


Fig. 17 The lowest three FVR for a Timoshenko beam carrying 'two' spring-mass systems under the effect of different temperature distributions: (a) mode A, (b) mode B, (c) mode C

6. Conclusions

This paper proposed a free vibration analysis method for Timoshenko beam carrying several spring-mass systems and considering the internal temperature distribution of the structure. Then, tests to measure the modal frequencies of a simply supported RC Timoshenko beam were conducted at varying temperatures to verify the correctness of the proposed method. The finite element models of Timoshenko beam carrying several spring-mass systems

were also established to illustrate the proposed method. Finally, the effect of different parameters of spring-mass systems and various temperature patterns on modal frequencies for Timoshenko beam have been discussed. In view of the results of this study the following conclusions could be drawn:

- The reliability of the proposed method was verified through the laboratory model and finite element models. The comparisons of *FVR* between theory and experimental results and comparisons between theory and FEM results both showed a reasonably accuracy of the proposed method.

- The modal characteristics especially frequencies are vulnerable to temperature for RC Timoshenko beam. It is mainly reflected on the effect of temperature on the elastic modulus and shear modulus of concrete, which lead to the variations of the shear coefficient and inertia of moment.

- The modal calculation results of Timoshenko beam under different temperature modes reveal that the influence of different temperature modes on frequency is different and the temperature has different effect on every frequency even in the same temperature mode.

- The modal calculation results of Timoshenko beam carrying single spring-mass systems illustrate that: (a) the frequencies increase with the stiffness while decrease with the mass; (b) the frequencies have suddenly changed when the frequency of the spring-mass system is equal to that of the bare beam.

The change of temperature does not produce secondary internal force for the simply supported beam, but not for other structures (e.g. rigid frame structures, continuous beam, etc.), which will be the topics the authors further deliberate from now on.

Acknowledgments

The present study has been sponsored by the National Natural Science Foundation of China (nos: 51378236 and 51478203) and transportation science and technology project of Jilin Province (nos: 2015-1-5 and 2015-1-8).

References

- Abramovich, H. and Elishako, I. (1990), "Influence of shear deformation and rotary inertia on vibration frequencies via love's equations", *J. Sound Vibr.*, **137**(3), 516-522.
- Abramovich, H. and Hamburger, O. (1991), "Vibration of a cantilever Timoshenko beam with a tip mass", *J. Sound Vibr.*, **148**(1), 162-170.
- Abramovich, H. and Hamburger, O. (1992), "Vibration of a cantilever Timoshenko beam with translational and rotational springs and with tip mass", *J. Sound Vibr.*, **154**(1), 67-80.
- Alvandi, A. and Cremona, C. (2006), "Assessment of vibration-based damage identification techniques", *J. Sound Vibr.*, **292**(1-2), 179-202.
- Askegaard, V. and Mossing, P. (1988), *Long Term Observation of RC-Bridge Using Changes in Natural Frequency*, Nordic concrete research, January.
- Baldwin, R. and North, M.A. (1973), *A Stress-strain Relationship for Concrete at High Temperatures*, Magazine of Concrete Research, December.
- Bruch, J.C. and Mitchell, T.P. (1987), "Vibrations of a mass-loaded clamped-free Timoshenko beam", *J. Sound Vibr.*, **114**(2), 341-345.
- Cornwell, P., Farrar, C.R., Doebling, S.W. and Sohn, H. (1999), "Environmental variability of modal properties", *Exp. Tech.*, **23**(6), 45-48.
- Cruz, P.J.S. and Salgado, R. (2009), "Performance of vibration-based damage detection methods in bridges", *Comput.-Aid. Civil Inf.*, **24**(1), 62-79.
- De Rosa, M.A., Auciello, N.M. and Maurizi, M.J. (2003), "The use of Mathematica in the dynamics analysis of a beam with a concentrated mass and dashpot", *J. Sound Vibr.*, **263**, 219-226.
- De Rosa, M.A., Franciosi, C. and Maurizi, M.J. (1995), "On the dynamics behaviour of slender beams with elastic ends carrying a concentrated mass", *Comput. Struct.*, **58**(6), 1145-1159.
- Doebling, S.W. and Farrar, C.R. (1997), "Using statistical analysis to enhance modal-based damage identification", *Proceedings of the Structural Damage Assessment Using Advanced Signal Processing Procedures Conference*, January.
- El-Sayed, T.A. and Farghaly, S.H. (2016), "Exact vibration of Timoshenko beam combined with multiple mass spring sub-systems", *Struct. Eng. Mech.*, **57**(6), 989-1014.
- Faires, J.D. and Burden, R.L. (2002), *Numerical Methods*, 3rd Edition, Brooks Cole, U.S.A.
- Faravelli, L., Ubertini, F. and Fuggini, C. (2011), "System identification of a super high-rise building via a stochastic subspace approach", *Smart Struct. Syst.*, **7**(2), 133-152.
- Farghaly, S.H. and El-Sayed, T.A. (2016), "Exact free vibration of multi-step Timoshenko beam system with several attachments", *Mech. Syst. Sign. Pr.*, **72-73**, 525-546.
- Farrar, C.R., Doebling, S.W., Cornwell, P.J. and Straser, E.G. (1997), "Variability of modal parameters measured on the Alamosa Canyon Bridge", *Proceedings of the 15th International Modal Analytical Conf. Bethel (CT): Society for Experimental Mechanics*, Washington, U.S.A., December.
- GB 50010-2010 (2010), *Code for Design of Concrete Structures*, Ministry of Housing and Urban-Rural Construction of the People's Republic of China; Beijing, China.
- Gürçöze, M. (1985), "On the vibration of restrained beams and rods with heavy masses", *J. Sound Vibr.*, **100**(4), 588-589.
- Gürçöze, M. (1996), "On the eigenfrequencies of cantilevered beams carrying tip mass and a spring mass in span", *J. Mech. Sci.*, **38**(12), 1295-1306.
- He, X., Conte, J.P.M. and Fraser, A. (2009), "Long-term monitoring of a highway bridge", *Proceedings of the 3rd International Operational Modal Analysis Conference*, Italy.
- Huang, T.C. (1961), "The effect of rotatory inertia and of shear deformation on the frequency and normal mode equations of uniform beams with simple end conditions", *J. Appl. Mech.*, **28**(4), 579-584.
- Kim, J.T., Park, J.H. and Lee, B.J. (2007), "Vibration-based damage monitoring in model plate-girder bridges under uncertain temperature conditions", *Eng. Struct.*, **29**(7), 1354-1365.
- Kukla, S. and Posiadala, B. (1994), "Free vibrations of beams with elastically mounted masses", *J. Sound Vibr.*, **175**(4), 557-564.
- Li, H., Li, S., Ou, J. and Li, H. (2010), "Modal identification of bridges under varying environmental conditions: Temperature and wind effects", *Struct. Contr. Hlth.*, **17**(5), 495-512.
- Liu, H., Wang, X. and Jiao, Y. (2016), "Effect of temperature variation on modal frequency of reinforced concrete slab and beam in cold regions", *Shock Vibr.*, **2016**(6), 1-17.
- Liu, W.H., Wu, J.R. and Huang, C.C. (1988), "Free vibrations of beams with elastically restrained edges and intermediate concentrated masses", *J. Sound Vibr.*, **122**(2), 193-207.
- Love, A.E.H. (1927), *A Treatise on the Mathematical Theory of Elasticity*, 4th Edition, Cambridge University Press, U.K.

- Maecck, J., Peeters, B. and De Roeck, G. (2001), "Damage identification on the Z24-bridge using vibration monitoring analysis", *Smart Mater. Struct.*, **10**(3), 512-517.
- Ni, Y.Q., Hua, X.G., Fan, K.Q. and Ko, J.M. (2005), "Correlating modal properties with temperature using long-term monitoring data and support vector machine technique", *Eng. Struct.*, **27**(12), 1762-1773.
- Peeters, B. and De Roeck, G. (2000), "One year monitoring of the Z24-Bridge: environmental influences versus damage events, #268", *Proceedings of the SPIE-The International Society for Optical Engineering Conference*, Texas, U.S.A.
- Peeters, B., Maecck, J. and De Roeck, G. (2001), "Vibration-based damage detection in civil engineering: Excitation sources and temperature effects", *Smart Mater. Struct.*, **10**(3), 518-527.
- Rayleigh, L. (1945), *Theory of Sound*, 2nd Edition, The Macmillan Company, New York, U.S.A.
- Register, A.H. (1994), "A note on the vibration of generally restrained end loaded beams", *J. Sound Vibr.*, **172**(4), 561-571.
- Roberts, G.P. and Pearson, A.J. (1996), "Dynamic monitoring as a tool for long span bridges", *Proceedings of the Bridge Management 3: Inspection, Maintenance, Assessment and Repair*, London, U.K., April.
- Rossi, R.E., Laura, P.A.A., Avalos, D.R. and Larrondo, H. (1993), "Free vibration of Timoshenko beams carrying elastically mounted, concentrated masses", *J. Sound Vibr.*, **165**(2), 209-223.
- Rossit, C.A. and Laura, P.A.A. (2001a), "Transverse vibrations of a cantilever beam with a spring mass system attached on the free end", *Ocean Eng.*, **28**, 933-939.
- Rossit, C.A. and Laura, P.A.A. (2001b), "Transverse normal modes of vibration of a cantilever Timoshenko beam with a mass elastically mounted at the free end", *J. Acoust. Soc. Am.*, **110**(6), 2837-2840.
- Salawu, O.S. (1997), "Detection of structural damage through changes in frequency: A review", *Eng. Struct.*, **19**(9), 718-723.
- Shoukry, S.N., William, G.W., Downie, B. and Riad, M.Y. (2011), "Effect of moisture and temperature on the mechanical properties of concrete", *Constr. Build. Mater.*, **25**(2), 688-696.
- Sohn, H., Dzwonczyk, M., Straser, E.G., Kiremidjian, A.S., Law, K.H. and Meng, T. (1999), "An experimental study of temperature effect on modal parameters of the Alamos Canyon Bridge", *Earthq. Eng. Struct. Dyn.*, **28**(8), 879-897.
- Su, H. and Banerjee, J.R. (2005), "Exact natural frequencies of structures consisting of two part beam-mass systems", *Struct. Eng. Mech.*, **19**(5), 551-566.
- Talebinejad, I., Fischer, C. and Ansari, F. (2011), "Numerical evaluation of vibration-based methods for damage assessment of cablestayed bridges", *Comput.-Aid. Civil Inf.*, **26**(3), 239-251.
- Timoshenko, S.P. (1921), *On the Correction for Shear of the Differential Equation for Transverse Vibrations of Prismatic Bars*, Philosophical Magazine, April.
- Timoshenko, S.P. (1922), *On the Transverse Vibrations of Bars of Uniform Cross Sections*, Philosophical Magazine, April.
- Wahab, M.A. and De Roeck, G. (1997), "Effect of temperature on dynamic system parameters of a highway bridge", *Struct. Eng. Int.*, **7**(4), 266-270.
- Xia, Y., Chen, B., Weng, S., Ni, Y.Q. and Xu, Y.L. (2012), "Temperature effect on vibration properties of civil structures: A literature review and case studies", *J. Civil Struct. Health Monitor.*, **2**(1), 29-46.
- Xia, Y., Hao, H., Zanardo, G. and Deeks A. (2006), "Long term vibration monitoring of a RC slab: Temperature and humidity effect", *Eng. Struct.*, **28**(3), 441-452.
- Xia, Y., Xu, Y.L., Wei, Z.L., Zhu, H.P. and Zhou, X.Q. (2011), "Variation of structural vibration characteristics versus non-uniform temperature distribution", *Eng. Struct.*, **33**(1), 146-153.
- Yan, A.M., Kerschen, G., De Boe, P. and Golinval, J.C. (2005a), "Structural damage diagnosis under changing environmental conditions-part 1: Linear analysis", *Mech. Syst. Sign. Pr.*, **19**(4), 847-864.
- Yan, A.M., Kerschen, G., De Boe, P. and Golinval, J.C. (2005b), "Structural damage diagnosis under changing environmental conditions-part 2: Local PCA for nonlinear cases", *Mech. Syst. Sign. Pr.*, **19**(4), 865-880.
- Zhou, G.D. and Yi, T.H. (2014), "A summary review of correlations between temperatures and vibration properties of long-span bridges", *Math. Probl. Eng.*, **2014**(1), 1-19.

CC